processes

MDPI

Article

Extended Kalman Filter Algorithm for Accurate State-of-Charge Estimation in Lithium Batteries

Gen Li [1], Qian Mao [2,*] and Fan Yang [3,*]

[1] School of Engineering, Hong Kong University of Science and Technology, Hong Kong; joker074lg@gmail.com
[2] School of Design, The Hong Kong Polytechnic University, Hong Kong
[3] Department of Electrical and Electronic Engineering, The Hong Kong Polytechnic University, Hong Kong
* Correspondence: vicky.mao@connect.polyu.hk (Q.M.); yangfan.yang@connect.polyu.hk (F.Y.)

Abstract: With the continuous development of the industrial and energy industries, the development of new energy vehicles is entering a period of rapid development and is one of the hot research directions today. Due to the needs of different working environments, the demand for mobile power sources in automobiles is increasing, which means that battery design and battery system management (BMS) determine their work efficiency. How to enable users to accurately and in real-time understand the usage status of their electric vehicle batteries is a very important thing, and it is also an important challenge faced in the development process of electric vehicles. This article proposes a battery state-of-charge (SOC) estimation method based on the extended Kalman filter algorithm (EKF) for one of the core areas of the BMS–battery state-of-charge (SOC). According to the guidance and direction of Industry 4.0 in Germany, we hope to address some of the aforementioned challenges for users of automotive and robotics products while developing our industry. Therefore, we made some innovative explorations in this direction. In this study, it was found that the algorithm can adjust parameters in real-time to achieve better convergence. The final estimation results indicate that the algorithm had high accuracy and robustness and can meet the current needs of battery estimation for new energy vehicles, providing an important means for the safety control of automotive BMS. In the long run, this will change the current situation of battery monitoring using mobile power sources. At the same time, it provided an effective and practical implementation method and template for current production estimation, which has a certain heuristic effect on the future process of Industry 4.0 and production estimation.

Keywords: production estimation; lithium battery; SOC estimation; enhanced extended Kalman filter; industry 4.0

Citation: Li, G.; Mao, Q.; Yang, F. Extended Kalman Filter Algorithm for Accurate State-of-Charge Estimation in Lithium Batteries. *Processes* **2024**, *12*, 1560. https://doi.org/10.3390/pr12081560

Academic Editor: Changhee Kim

Received: 30 June 2024
Revised: 17 July 2024
Accepted: 23 July 2024
Published: 25 July 2024

1. Introduction

The burgeoning proliferation of portable electronic devices, ranging from smartphones to electric vehicles, especially in the process of industrial production operations and when users use industrial products, means that efficient energy technology is particularly important, underscoring the indispensability of batteries as a primary power source [1]. As such, the state-of-charge (SOC) estimation assumes paramount importance in ensuring efficient and optimal utilization of battery resources [1,2]. While conventional SOC estimation methods, such as the discharge test method and open circuit voltage method, have served as stalwarts in the field, emerging methodologies, including the least squares method, Kalman filtering method, and neural network method, present promising avenues for enhanced accuracy and versatility [3]. The estimation method is related to various mathematical models and physical models. This project studies batteries in real life from a more professional and deeper perspective. There are all kinds of portable (non-wire connected) electronic devices in our life, with small power electronic devices that include all kinds of electric toys, smart phones, portable computers, etc., and large power devices

that include all kinds of batteries used in electric vehicles and aerospace equipment [4,5]. These devices all need a large number of batteries as their power supply for mechanical movement or operation calculation. It can be seen that battery is an indispensable and important energy supply device in real life, and a relatively complete battery management system (BMS) has also been derived, which provides a good environment for the human management, control, and upgrading of batteries [6].

At present, most SOC estimation methods in the world are based on the discharge test method, open circuit voltage method, and ampere hour integration method, which are more traditional methods and have a relatively fixed range of use [7]. However, relatively new methods include the least squares method, Kalman filtering method, neural network method, etc. [8]. The purpose of these algorithms is to develop a model that can describe the behavior of lithium batteries based on one or more algorithms in order to meet the requirements of BMS management [9]. The OCV method can estimate the SOC value by measuring the open-circuit voltage of the battery [10]. Since this method requires a long time to obtain a stable OCV value, it is not suitable for SOC estimation in cases where the battery current changes drastically. The Ah integral method is currently the most commonly used for EVs, and it estimates the SOC by the integration of the load current against time [11]. The drawback is that it cannot automatically determine the initial value of SOC and has a large cumulative error [11].

This paper proposed the self-adaptive parameter system for the modified EKF method. Firstly, the voltage estimation error caused by the EKF method when performing SOC estimation decreased through the modified EKF method. We established an accurate battery model and improved the accuracy of battery voltage estimation without affecting the battery SOC estimation. Specifically, the Kalman gain and noise were focused on and studied in the estimation of the battery voltage. By designing the Kalman gain formula and voltage estimation formula at the points where the current changes, the error of the estimated voltage can be effectively reduced. The self-adaptive parameter system based on the modified EKF method was tested under the working current, and the errors of the SOC and voltage were both reduced. This means that in the production estimation direction related to batteries, our proposed improved EKF method for estimating batteries can effectively achieve real-time monitoring and accurate estimation of batteries, providing an effective solution for BMS to monitor battery SOC.

2. Materials and Methods

2.1. Experimental Materials

The battery itself is a closed and complex chemical system, especially lithium-ion batteries [12,13]. Its working principle is different from ordinary dry batteries, and its basic components include the positive and negative electrode materials, the electrolyte, and the separator [14]. The positive and negative electrode materials can ensure the reversible insertion and removal of lithium ions in it, achieving the purpose of storing and releasing energy [15]. The separator is used to form a channel for the movement of lithium ions, and the electrolyte ensures the movement of lithium ions [16–18]. By ensuring that electrons can move in one direction externally to form a stable current, power can be supplied to the device [19].

The materials we prepared during the experiment included (1) a lithium polymer battery (model: 103565, Guangzhou Shengyuan Technology Co., Guangzhou, China); (2) a battery charge and discharge tester (GeLingDe Co., Foshan, China); and (3) the BTS 8.0 software. This set of experimental equipment is often used to measure the parameters of lithium batteries in small electrical appliances and is widely applicable for measuring batteries in underwater robots, drones, and small, self-programming robots.

2.2. Overall Experimental Methods

Due to the discharge characteristics of lithium batteries [20], we can divide the entire discharge experiment process of lithium batteries into the following three steps.

In the initial stage, the terminal voltage of the battery drops rapidly, and the larger the discharge rate, the faster the voltage drops. Then, the battery voltage enters a stage of slow change, which is called the platform area of the battery. The lower the discharge rate, the longer the platform area lasts; the higher the platform voltage, the slower the voltage drop. When the battery is nearly discharged, the battery load voltage starts to drop sharply until it reaches the discharge cutoff voltage.

Here, the constant current discharge method was adopted because it can obtain the HPPC curve for the subsequent calculation. During discharge testing, the device applied a certain load to the battery and recorded the evolution of voltage over time and the current over time, based on the set data recording conditions.

2.2.1. Experimental Model

In the equivalent circuit of a battery cell, the circuit typically consists of a voltage source, a series resistor, and one or more parallel resistor capacitor pairs. The voltage source provides open circuit voltage, while other components simulate the internal resistance and time-dependent behavior of the battery. Here, we considered the efficiency and computational burden of the algorithm, so we adopted a second-order RC equivalent circuit model. Figure 1 shows the schematic diagram of the second-order RC circuit model, which is characterized by its physical model containing two sets of parallel capacitors and resistors. At the same time, it included the open circuit voltage and the internal resistance R_0 of the battery. The main reasons for this are as follows.

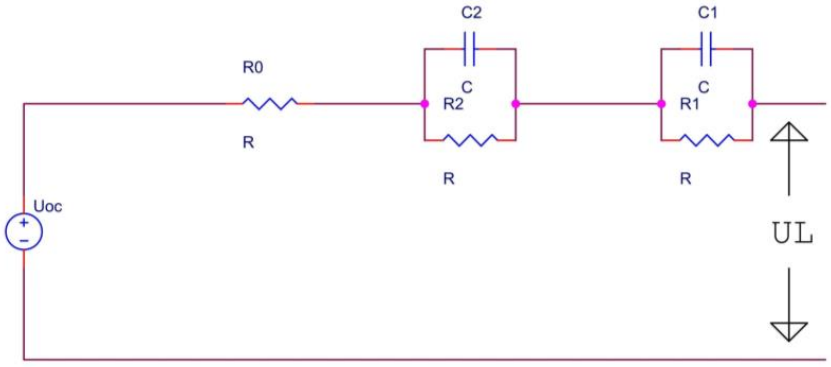

Figure 1. Second-order RC Model.

When dealing with complex power devices such as lithium battery packs, we usually break them down into small battery cells or cells, which can significantly reduce computational complexity and avoid the accumulation of errors caused by the mutual influence between battery cells. The higher the order, the higher the complexity of the calculation, which is not conducive to the online estimation of SOC. At the same time, it is also possible to fit too much noise data, resulting in over fitting. It is much more accurate than the first-order model but not much different from the third-order model.

2.2.2. Offline Parameter Identification

In order to gain a deeper understanding of the characteristics of resistance and capacitance in the equivalent circuit model in Figure 1, we used a typical pulse current discharge mode to analyze the voltage response curve of the pulse current discharge. Figure 2 shows a partially enlarged image of the pulse current discharge experiment. The diagram is divided into four stages from the discharge state to the static state.

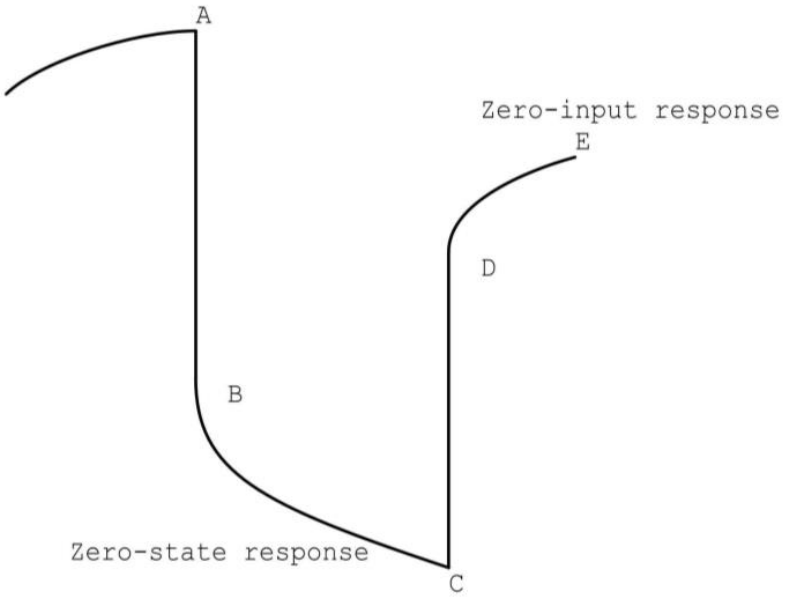

Figure 2. Discharge current curve (one-pulse cycle).

Phase AB: When the battery changes from a stationary state to a discharging state, the voltage value drops sharply. Phase BC: As the battery continues to load current pulses, the capacitors gradually charge. Due to the presence of their respective resistances, the voltage exponentially decreases slowly, resulting in a zero-state response. Phase CD: The battery experiences a sharp increase in voltage when the current pulse is removed. Phase DE: When the battery loses its pulse and slowly recovers, the capacitors will produce a slow discharge effect through their respective resistors, causing the voltage to slowly rise. This state is the zero-input state. The AB and CD phases are based on a second-order equivalent circuit, and the terminal voltage of the capacitor will not suddenly change.

The overall experimental process can be divided into the following steps: (1) Determining the physical model of the battery corresponding to the experiment: this step is crucial, as it will directly affect the number of parameters and results in the subsequent parameter identification; (2) offline parameter identification: it is mainly carried out by centrally processing the data to obtain the estimated model parameters and then inputting them into the online parameter identification algorithm. The relationship between SOC and OCV is identified during the estimation of battery capacity in real-time; (3) online parameter identification: the principle of online parameter identification is to use the recursive real-time updating of model parameters during system operation using EKF; (4) this step compares the estimated data with the original data and analyzes the robustness, convergence, and accuracy of EKF in the production estimation process.

Based on this characteristic, we can use calculations and fitting to obtain the parameters we need:

$$U_L = U_{OC} - U_0 - U_1 - U_2 \tag{1}$$

$$\tau = RC \tag{2}$$

$$U_0 = I_L * R_0 \tag{3}$$

$$U_p = U_{c1} + U_{c2} = I_L * R_1 * \left(1 - e^{-t/\tau_1}\right) + I_L * R_2 * \left(1 - e^{-t/\tau_2}\right) \tag{4}$$

$$U_p{}' = U_{01} * e^{-t/\tau_1} + U_{02} * e^{-t/\tau_2} \tag{5}$$

At point B, the battery begins to load the current for a short period of time, so we consider point B as the time t = 0. At this point, we can use Formulas (1), (3), and (4) to obtain a new formula:

$$U_L = U_{OC} - U_0 - U_1(0) * e^{-t/\tau_1} - U_2(0) * e^{-t/\tau_2} \quad (6)$$

Finally, using the fitting formula in Matlab R2021a, we can obtain the parameters R_1, R_2, C_1, C_2, and R_0 using the recursive least square method [9] or other methods. By importing experimental data into Cftool in Matlab and selecting an appropriate fitting function, we can approximate the previously obtained data into a continuous function curve. By comparing this curve with the standard HPPC curve, we can see that it conforms to a certain segment of "zero correspondence".

In the actual operation, we only need to perform the following steps to achieve the above parameter identification: (1) selecting the zero-response state or zero-input state in the pulse curve; (2) realizing the fitting of experimental data through Cftool in MATLAB; and (3) obtaining the parameter identification results of resistance and capacitance in the lithium battery.

Finally, the main parameters are obtained, including open circuit voltage, resistance, and capacitance.

2.2.3. Online Parameter Identification

Our idea is that the initial SOC value is calculated using the open-circuit voltage method, and we hope to achieve the optimal estimation and approximate the true value through a period of iteration under the special algorithm.

The relationship between the variables of the classical Kalman filter algorithm is linear, so the classical Kalman filter algorithm is only applicable to the state estimation of linear systems. Lithium batteries are a complex system, and the relationship between their parameters is not a simple linear relationship. Therefore, SOC estimation requires the use of a derivative algorithm of the Kalman filtering algorithm. The basic idea of the EKF algorithm is to linearize the equation through Taylor expansion.

Scheme 1 represents the process of reproducing EKF in MATLAB. It strictly followed the following process [3]: (1) preparing the experimental equipment; (2) initializing the experimental data; (3) importing the existing data; and (4) using the extended Kalman algorithm to process the data for accurate estimation.

Overall, based on the voltage difference and filtering gain, the extended Kalman filtering method was used to correct the Kalman filtering gain. At the same time, the initial value of SOC (t1) was used to obtain the corrected value of SOC at time t2, represented by SOC (t2). At the next moment, the corrected SOC value SOC (t2) was used as the initial value to calculate the SOC and input it, and then the extended Kalman filter method was used to correct it so as to continuously cycle it. To put it another way, it meant the Kalman filtering algorithm of this algorithm followed the order of "prediction correction prediction".

Materials and equipment	1. Computer with MATLAB program; 2. Obtained experimental data; 3. Obtained offline parameter identification results.
Process	A) Complete initialization 1. Import the data in the experiment table and name it; 2. Specify sampling frequency and step size; 3. Define the state vector and the EKF covariance and set the initial value of the state vector.
	B) Input data 1. Create the dynamic estimated mathematical battery model; 2. Input parameters and formulas obtained through offline parameter identification; 3. Input the experimental data obtained through the experiment; 4. Use the above formula and data to complete the definition of the matrix (transfer matrix, input matrix, and output matrix); 5. Define the Jacobian matrix.
	C) Extended Kalman filter 1. Covariance forecast update; 2. State vector prediction update; 3. Obtain the open-circuit voltage formula about the SOC function; 4. Voltage adjustment; 5. Kalman gain update; 6. Kalman gain adjustment; 7. Predicted terminal voltage; 8. State vector measurement update; 9. Update covariance matrix. Start cycle 1~9

Scheme 1. Process of writing EKF using Matlab.

3. Results

3.1. Overall Experimental Results

3.1.1. Offline Parameter Identification

In this step, we identify several parameters in the battery that cannot be measured. The usual method used is to obtain these parameters through experiments and calculations. Through offline parameter identification, we can easily obtain the parameters of various required data in Table 1. These parameters represent the internal state of the battery under a fixed SOC state, but the internal state of the battery itself is a constantly changing physical and chemical state. Therefore, these parameters are far from meeting our BMS and production estimation needs under actual conditions. The data volume of these parameters is small and cannot cover the entire battery charging and discharging process.

Table 1. Offline parameter identification results.

SOC (%)	R0 (Ω)	R1 (Ω)	R2 (Ω)	C1 (F)	C2 (F)
SOC 10–0	-	9.75142857	0.05325714	-	-
SOC 20–10	0.20521368	9.93428571	0.06350000	6244.50929488	984.25196850
SOC 30–20	0.20300456	10.15857143	0.08502857	7180.09030606	1483.44511677
SOC 40–30	0.20055294	10.42142857	0.05954286	6654.37824908	1121.88543179
SOC 50–40	0.22932802	10.46857143	0.05154286	16,370.8684583	967.64734671
SOC 60–50	0.23516314	10.48714286	0.05085714	44,309.87744453	1068.63708984
SOC 70–60	0.21807398	10.56714286	0.06392857	27,398.07738339	1691.25942806
SOC 80–70	0.26893139	10.69428571	0.06467143	10,590.99347786	1748.78743957
SOC 90–80	0.24105345	10.88571429	0.05437143	11,069.22725921	1372.53821854
SOC90-	0.19391196	11.14000000	0.11275714	8681.49002150	890.96021572

3.1.2. Online Parameter Identification

Through the experimental ideas and ideas of online parameter identification mentioned above, we obtained the formation results of the following Kalman filter.

The state equation and initial equation are as follows:

$$x_k = Ax_{k-1} + \Gamma w_{k-1} \tag{7}$$

$$z_k = Hx_k + v_k \tag{8}$$

$$x_{k+1} = f(x_k, u_k, k) + \Gamma w_k \tag{9}$$

$$y_k = g(x_k, u_k, k) + v_k \tag{10}$$

The state variables of the system at the next moment, the output variables of the system, and the error covariance can be estimated, using the measured output values of the system to correct the current state estimation of the system.

x_{k-1} is the system state variable, and z_k is the system output. A is the transfer matrix, Γ is the noise coefficient matrix, H is the measurement matrix, w_{k-1} is the state noise, v_k is the measurement noise, and both represent the Gaussian white noise.

We generally set the expected white noise to zero, that is:

$$E\left[v_k v_j^T\right] = R_k \delta_{kj} \tag{11}$$

$$E\left[w_k w_j^T\right] = Q_k \delta_{kj} \tag{12}$$

After algorithm initialization, the following steps were cycled through:

1. The estimates were calculated as:

$$\text{Prior state estimation}: \ \hat{x}_{k/k-1} = f[\hat{x}_{k-1}, k] \tag{13}$$

$$\text{Estimation bias}: \ \widetilde{x}_k = \hat{x}_k - x_k = f\left[\widetilde{x}_{k-1}, k\right] - \Gamma w_{k-1} \tag{14}$$

The error covariance matrix was further estimated as:

$$P_{k/k-1} = A P_{k-1} A^T + \Gamma Q_{k-1} \Gamma^T \tag{15}$$

2. The estimated values were corrected through measured values.
   (1) The Kalman gain for determining the weight during correction was calculated by calculating the Kalman gain:

$$K_k = P_{k/k-1} H^T (H P_{k/k-1} H^T - R_k)^{-1}. \tag{16}$$

   (2) The next moment system state estimator was updated:

$$\hat{x}_k = \hat{x}_{k/k-1} + K_k\{y_{k+1} - g[\hat{x}_{k/k-1}, k+1]\} \tag{17}$$

   (3) The error covariance matrix was updated:

$$P_k = (I - K_k H) P_{k/k-1} \tag{18}$$

x_k is the value of the state variable at time k, and y_k is the value of the output at time k. The u_k in the equation is the output value of the system at time k. v_k and w_k are both the Gaussian white noise, w_k is the process noise, v_k is the measurement noise, and gamma is the noise matrix. We abbreviated the transfer matrix, input matrix, output matrix, and feedforward matrix related to x_k and u_k here.

The entire process is shown in a flow diagram.

We can simplify the entire process mentioned above into a flowchart that can accommodate EKF for production estimation in most cases [3]. The EKF flowchart in Figure 3 provides an overview of the EKF algorithm on images, making it not only applicable for production estimation in our BMS but also expandable to other production estimation environments.

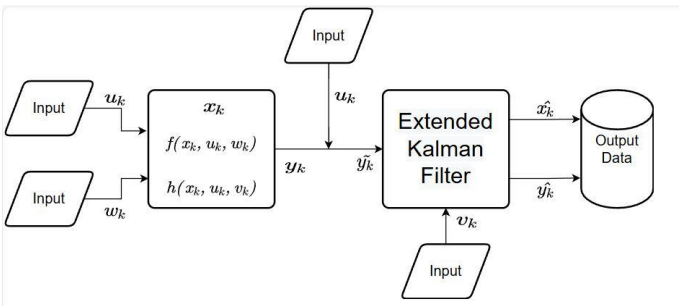

Figure 3. Enhanced EKF process.

3.2. Kalman Gain Derivation

w_k and v_k are independent of each other, and in reality, both types of noises cannot be removed and cannot be measured [4]. To address this mathematical characteristic, we can use the product of their Gaussian distributions to obtain a new Gaussian distribution map.

We can assume the distributions of noises w_k and v_k to be:

$$v_k = \left(\frac{1}{\sigma_1 * \sqrt{2\pi}}\right) * exp\left(-\frac{(x-\mu_1)^2}{2 * {\sigma_1}^2}\right) \tag{19}$$

$$w_k = \left(\frac{1}{\sigma_2 * \sqrt{2\pi}}\right) * exp\left(-\frac{(x-\mu_2)^2}{2 * {\sigma_2}^2}\right) \tag{20}$$

Their product can be obtained, and a new normal distribution can be constructed as:

$$v_k * w_k = \left(\frac{1}{2 * \pi * \sigma_1 * \sigma_2}\right) * exp\left(-\left(\frac{(x-\mu_1)^2}{2 * {\sigma_1}^2} + \frac{(x-\mu_2)^2}{2 * {\sigma_2}^2}\right)\right) \tag{21}$$

The function related to probability density mentioned above can be simplified as:

$$v_k * w_k = S_g * \left(\frac{1}{\sqrt{2\pi\left(\frac{{\sigma_1}^2 * {\sigma_2}^2}{{\sigma_1}^2 + {\sigma_2}^2}\right)}}\right) * exp\left(-\frac{\left(x - \left(\frac{\mu_1 * \sigma_2 + \mu_2 * \sigma_1}{{\sigma_1}^2 + {\sigma_2}^2}\right)\right)^2}{2 * \left(\frac{{\sigma_1}^2 * {\sigma_2}^2}{{\sigma_1}^2 + {\sigma_2}^2}\right)}\right) \tag{22}$$

$$S_g = \left(\frac{1}{\sqrt{.2\pi({\sigma.}_1{}^2 + {\sigma_2}^2)}}\right) * exp\left(-(\frac{(\mu_1 - \mu_2)^2}{.2 * ({\sigma.}_1{}^2 + {\sigma_2}^2)})\right) \tag{23}$$

The distribution center and variance of the new Gaussian distribution can be calculated as:

$$\mu' = \frac{\mu_1 * \sigma_2 + \mu_2 * \sigma_1}{{\sigma_1}^2 + {\sigma_2}^2} \tag{24}$$

$$\sigma'^2 = \frac{{\sigma_1}^2 * {\sigma_2}^2}{{\sigma_1}^2 + {\sigma_2}^2} \tag{25}$$

Among them, S_g can be regarded as a constant term, which is called the scaling factor; it controls the compression or amplification of the new Gaussian distribution.

Figure 4 shows the image description of the above process. It is obvious that the red and green curves are two independent Gaussian distributions. From the blue curve, it can be roughly seen that the product result is a compressed Gaussian distribution with an expected value between [μ_1, μ_2], and the variance and the mean properties of the new Gaussian distribution remain unchanged. Finally, after fusing two different Gaussian distributions, the result is still conforming to the Gaussian distribution.

The above steps show the derivation of the Kalman gain coefficient; its expression form is similar to that of the Kalman gain coefficient, which helps better understand the significant impact of the gain coefficient on prediction. It is a very important breakthrough for using Kalman filtering to estimate battery SOC. The smaller the variance in the one-dimensional error is, the more accurate it is; the smaller the covariance in the multi-dimensional error is, the smaller the trace of the covariance matrix is, and the more accurate it is.

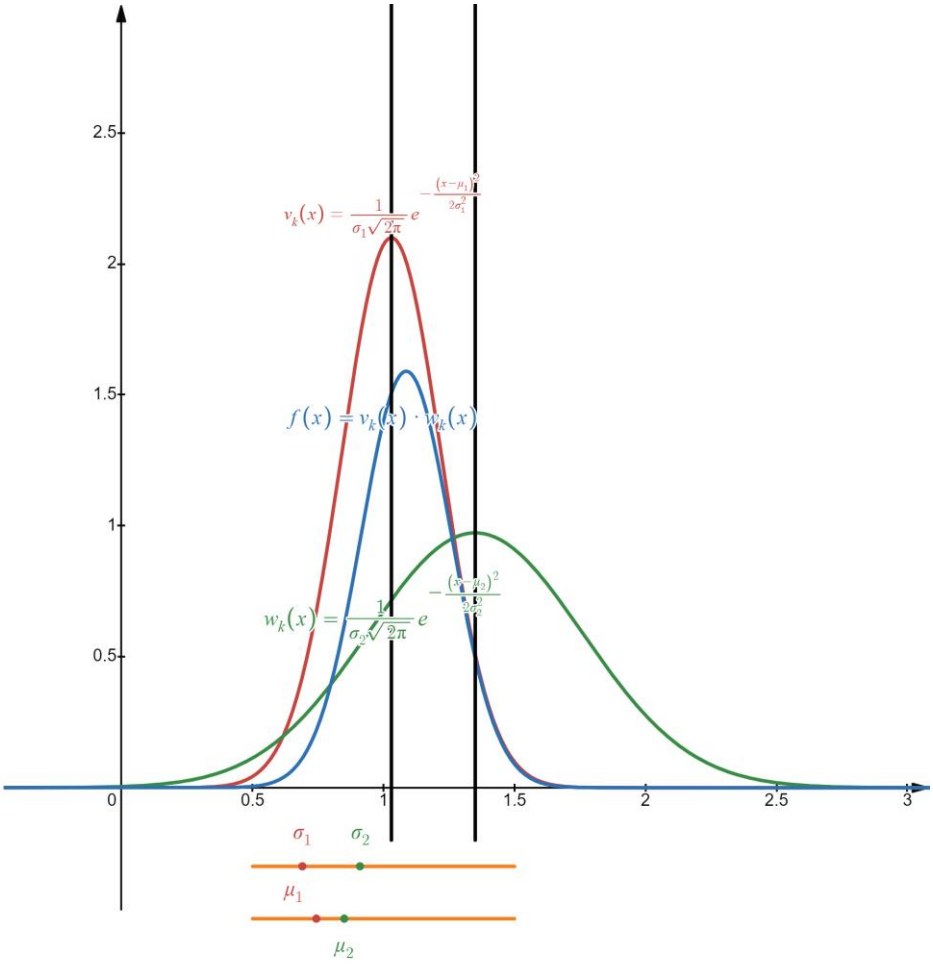

Figure 4. Gaussian distribution map of noise.

We tried different Kalman weights, adjusted for covariance, and compared them. We extracted several sets of data with significant differences and unique features, which are shown in Table 2. The unique feature was that we identified various errors.

Table 2. Results of changing Kalman gain coefficient and covariance adjustment.

Kalman Gain (R)	Covariance Adjustment (Q)	Maximum Error	Minimum Error	Integral Error
0.10000000	0.10000000	0.03853000	−0.04135000	0.07988000
1.00000000	0.10000000	0.04068000	−0.06665000	0.10733000
10.00000000	0.10000000	0.03969000	−0.11860000	0.15829000
0.100000000	1.00000000	0.03734000	−0.03922000	0.07656000
1.00000000	10000000	0.03853000	−0.04127000	0.07980000
10.00000000	1.00000000	0.04036000	−0.06665000	0.10701000
0.10000000	10.00000000	0.03756000	−0.04023000	0.07779000
1.00000000	10.00000000	0.03758000	−0.04030000	0.07788000
10.00000000	10.00000000	0.03782000	−0.04135000	0.07917000

3.3. Final Simulation Results

By incorporating the results of offline parameter identification into the initial state of online parameter identification, we can simulate the charging and discharging states of the battery in this way and obtain the following simulation results graph. Figure 5a shows the original experimental results and estimation results. The blue curve represents the original experimental results, and the red curve represents the estimation results. Figure 5b shows the estimation error.

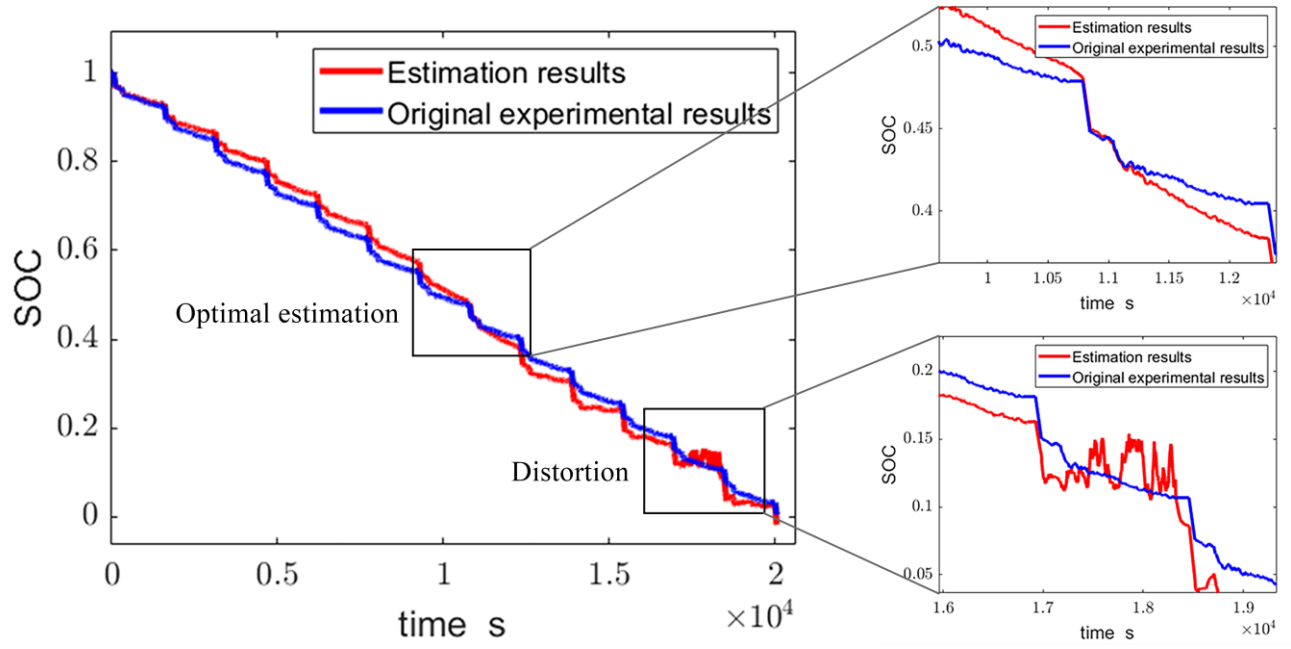

(**a**)

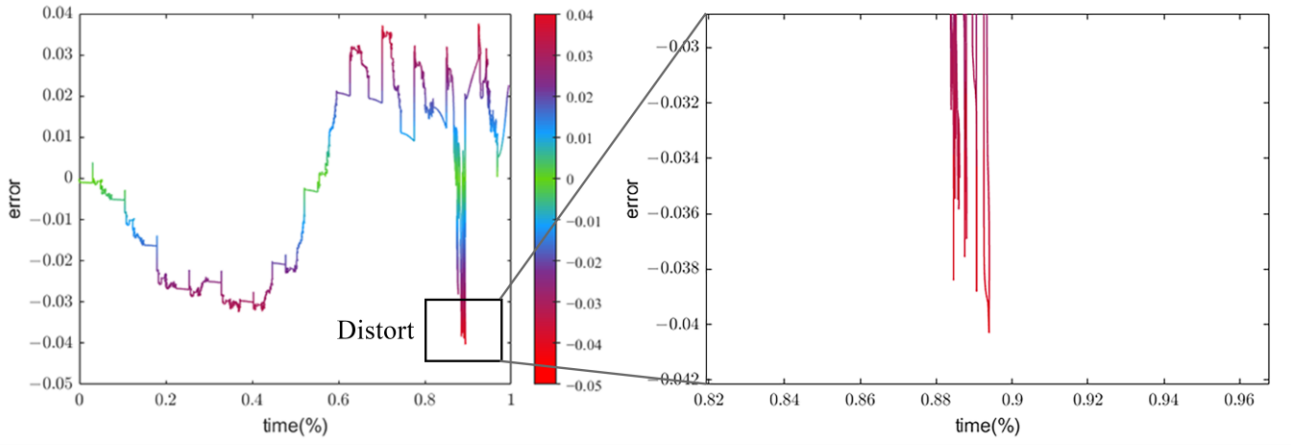

(**b**)

Figure 5. (**a**) Estimated curve by EKF and original curve. (**b**) Error curve.

In Figure 5a, the optimal estimation result and the distorted area in the image are extracted. It is not difficult to find that during the optimal estimation period, the overlap between the two curves is high and tends to be stable. However, in the distorted area, the estimation result fluctuates greatly, and the blue curve representing the true value also shows a rapid downward trend. In Figure 5b, the curve in the green area represents a small error between the simulation results and the actual results, indicating a good estimation result. The curve in the red area represents a large error and poor estimation results. At the same time, the distortion area in the figure is marked, corresponding to the distortion area in Figure 5a.

4. Discussion

4.1. Discussion of Offline Parameter Identification

In this experiment, the discharge experimental images of lithium batteries at 0–100 SOC were successfully obtained. A constant current discharge method for 30 min was adopted. The battery was then left to stand for 30 min to stabilize its internal chemical state at the beginning of the next discharge cycle. This process was repeated 10 times at an ambient temperature of 298 K to obtain complete discharge data for the entire battery, and data from 10 experiments were recorded for fitting and programming purposes. From Table 1 and Figure 5a, it can be concluded that:

1. When the SOC was lower than 10%, the discharge curve did not conform to the general HPPC curve.
2. The RMSE of the offline parameter identification of this section was between 0.001975 and 0.0007406, with high stability.
3. Only the partial discharge time period was selected for this curve, and partial voltage sudden change was excluded.

By analyzing the SSE, R-square, Adjust-square, and RMSE of the fitted curve and the original curve, the reasons for the significant difference between the experimental parameters and the fitted curve during offline parameter identification were obtained and will be explained in the following section.

4.2. Discussion of Online Parameter Identification

Through existing experiments and simulations, the following conclusions can be drawn:

1. The prediction data of the extended Kalman filter algorithm needed to reach the best state at 1–1.2 $\times$ 10^4 (S), that is, when the SOC was between 0.5–0.4, the line estimation effect was the best.
2. The difference between the SOC estimated by this technology and the original SOC fluctuated between (0.03756, $-$0.04023), which meant that it had a good accuracy in SOC estimation.

However, from the perspective of segmentation, the estimation results in the first half of the experiment were significantly more stable, and the results in the second half fluctuated greatly, indicating that the robustness of EKF estimation was poor in this period. On the other hand, after crossing 1.2 $\times$ 10^4 (S), the convergence of the algorithm decreased. From Table 2, it can be seen that the optimization of SOC estimation came from reducing the increasing error in transmission, that is, timely suppressing the covariance of state estimation. Moreover, from previous experiments, it can be concluded that state prediction based solely on state equations is usually not suitable for a long time. The transmission of errors accelerated the accumulation of errors. Through repeated experiments, we found that, by modifying the covariance matrix, the original EKF model can achieve better convergence with high volatility data. This fluctuation in data is usually caused by the rapid decline in battery power when it is about to run out. The robustness of the original EKF rapidly decreased when it crossed the point of power decline.

At the same time, in the experiment, it was found that the Kalman gain seriously affected the convergence of the estimation curve. High weight will generally make the low error data have better convergence, while high error data will magnify its error. Based on this principle, we propose maintaining the correction of the estimated value by changing the Kalman gain in the EKF method calculation to ensure data with a high robustness of estimated data.

5. Conclusions

This article focuses on lithium batteries and establishes a second-order RC model that includes internal resistance in the estimation model using EKF. Meanwhile, EKF was used to estimate SOC values. A second-order RC model with high accuracy was obtained through the offline parameter identification method. At the same time, under HPPC conditions, the

EKF algorithm was used in conjunction with existing equivalent circuit models to estimate the battery SOC. In particular, the noise variance caused by current and voltage accuracy issues was analyzed, and the maximum error was only 7.7779%, which demonstrates better stability in estimation accuracy [5,9]. Moreover, better estimation results were obtained by adjusting the relevant noise matrix. This indicates that the extended Kalman filtering algorithm can be used to solve the problem of the real-time performance of algorithms, such as the open voltage method and the low accuracy of the ammeter integration method. The EKF algorithm has high accuracy, good convergence, and robustness when used for SOC estimation. It was also explicitly stated in other literature that the algorithm has a strong adaptability and low computational complexity. Through constant correction, the algorithm has a good convergence and a good suppression of Gaussian white noise.

This research achievement largely interprets some of the ideas in the Industry 4.0 process [20,21], using models and simulations to create transparency in product architecture for engineers, and can explain and describe existing systems. Estimating from the production end to the user end can enable products to achieve end-to-end matching in the overall architecture of Industry 4.0. This industrial estimation is no longer limited to estimating the economic value of the product but is more representative of the product's own value. It can reflect the excellent performance of the product at a deeper level.

Returning to the value of research, the estimation of battery SOC is of great significance for battery management, as it is an important part of the development of new energy and an indispensable part of various industrial industries. Mobile phones, laptops, and intelligent robots are all inseparable from lithium-ion batteries at present. Whether it is a small capacity battery or a large storage battery, estimating their SOC is very important because this method allows us to know the charge state of the battery in real-time, without the needs for measurement instruments. In both the Kalman filtering algorithm and the neural network algorithm, we can estimate the next state of the battery based on the observed state at the current stage and improve its estimation accuracy through correction. Because of this advantage, there will be more and more Kalman algorithms in the future, and their types will also become more and more diverse. Due to its excellent performance in BMS, extended Kalman filtering algorithms, double-extended Kalman filtering algorithms, and adaptive extended Kalman algorithms are emerging.

Industry 4.0 emphasizes decision-making by data-driven and intelligent manufacturing. In the future, this also means that production estimation will increasingly rely on big data analysis and machine learning algorithms. In this study, we optimized the production process in Industry 4.0 using EKF. The future development strategy aims to incorporate production estimation controlled by digital twin technology to enhance efficiency, accuracy, and adaptability in manufacturing processes. Digital twin technology, which creates a virtual replica of physical assets, processes, and systems, will play a pivotal role in revolutionizing production estimation and management [22] in Industry 4.0, based on this initial concept. This technology allows for the continuous monitoring of equipment performance, identifying potential issues before they cause disruptions and providing insights for proactive maintenance. The real-time feedback loop between the physical and digital counterparts will ensure that production estimation is always based on the most current and accurate data, reducing downtime and improving overall productivity.

Furthermore, digital twin technology will facilitate advanced analytics and machine learning applications, enabling predictive modeling and decision-making processes that adapt to changing conditions. This adaptive capability will enhance our ability to respond to market demands swiftly and efficiently, ensuring that production schedules and resource allocations are optimized for maximum output and minimal waste. Implementing this strategy involves several key steps.

(1) The first step is the monitoring of production equipment. One idea of digital twin technology is to "monitor the status of production equipment in real-time during production, predict potential faults and maintenance needs, reduce downtime and maintenance costs." For industrial production in highly complex environments, it is difficult for a single

sensor and traditional physical monitoring methods to monitor the status of the entire equipment in real-time, accurately and comprehensively. In the future, combining EKF, UKF, PF, and other algorithms with deep learning models can achieve data fusion [23] between multiple sensors and improve data reliability and real-time performance. (2) The second step is to dynamically optimize the production process. Through the digital twin model, the implementer can simulate different production strategies, evaluate their effectiveness, and find the optimal production plan. The production process can be estimated and dynamically adjusted based on real-time data to optimize the production process. (3) The final step is the virtual simulation of products. In the process of developing new products, we hope to use real-time production data and user feedback historical data to achieve virtual simulation, test product performance and reliability, and reduce the development cost of physical prototypes through estimation and simulation.

Author Contributions: Conceptualization, F.Y. and Q.M.; methodology, F.Y.; software, F.Y.; validation, F.Y. and Q.M.; formal analysis, Q.M.; investigation, Q.M.; resources, F.Y.; data curation, G.L.; writing—original draft preparation, F.Y. and Q.M.; writing—review and editing, G.L., Q.M., and F.Y. All authors have read and agreed to the published version of the manuscript.

Funding: This research was funded by the Hong Kong Polytechnic University.

Data Availability Statement: The details about data supporting the reported results are available upon request from the corresponding author.

Acknowledgments: We acknowledge the funding received from Hong Kong Polytechnic University.

Conflicts of Interest: All co-authors have seen and agreed with the content of the manuscript, and there is no financial interest to report. We declare that the manuscript is original and has not been published before or submitted elsewhere for consideration of publication. We know of no conflicts of interest associated with this work, and there has been no significant financial support for this work that could have influenced its outcome.

References

1. Yang, F.; Shi, D.; Mao, Q.; Lam, K.-h. Scientometric research and critical analysis of battery state-of-charge estimation. *J. Energy Storage* **2023**, *58*, 106283. [CrossRef]
2. Klintberg, A.; Klintberg, E.; Fridholm, B.; Kuusisto, H.; Wik, T. Statistical modeling of OCV-curves for aged battery cells. *Int. Fed. Autom. Control Pap.* **2017**, *50*, 5. [CrossRef]
3. Qiu, Y.; Li, X.; Chen, W.; Duan, Z.M.; Yu, L. State of charge estimation of vanadium redox battery based on improved extended Kalman filter. *ISA Trans.* **2019**, *94*, 326–337. [CrossRef] [PubMed]
4. Zarchan, P.; Musoff, H. *Progress in Astronautics and Aeronautics: Fundamentals of Kalman Filtering: A Practical Approach*; AIAA: Reston, VA, USA, 2009; Volume 208.
5. Ramadan, H.S.; Becherif, M.; Claude, F. Extended kalman filter for accurate state of charge estimation of lithium-based batteries: A comparative analysis. *Int. J. Hydrogen Energy* **2017**, *42*, 29033–29046. [CrossRef]
6. Li, Y.; Wang, C.; Gong, J. A combination Kalman filter approach for State of Charge estimation of lithium-ion battery considering model uncertainty. *Energy* **2016**, *109*, 933–946. [CrossRef]
7. Shrivastava, P.; Soon, T.K.; Idris, M.Y.I.B.; Mekhilef, S. Overview of model-based online state-of-charge estimation using Kalman filter family for lithium-ion batteries. *Renew. Sustain. Energy Rev.* **2019**, *113*, 109233. [CrossRef]
8. Lee, J.; Nam, O.; Cho, B.H. Li-ion battery SOC estimation method based on the reduced order extended Kalman filtering. *J. Power Sources* **2007**, *174*, 9–15. [CrossRef]
9. Peng, J.; Luo, J.; He, H.; Lu, B. An improved state of charge estimation method based on cubature Kalman filter for lithium-ion batteries. *Appl. Energy* **2019**, *253*, 113520. [CrossRef]
10. Lavigne, L.; Sabatier, J.; Francisco, J.M.; Guillemard, F.; Noury, A. Lithium-ion Open Circuit Voltage (OCV) curve modelling and its ageing adjustment. *J. Power Sources* **2016**, *324*, 694–703. [CrossRef]
11. Hannan, M.A.; Hoque, M.M.; Hussain, A.; Yusof, Y.; Ker, P.J. State-of-the-Art and Energy Management System of Lithium-Ion Batteries in Electric Vehicle Applications: Issues and Recommendations. *IEEE Access* **2018**, *6*, 19362–19378. [CrossRef]
12. Deng, Z.; Lin, X.; Huang, Z.; Meng, J.; Zhong, Y.; Ma, G.; Zhou, Y.; Shen, Y.; Ding, H.; Huang, Y. Recent progress on advanced imaging techniques for lithium-ion batteries. *Adv. Energy Mater.* **2021**, *11*, 2000806. [CrossRef]
13. Fanga, L.; Lia, J.; Peng, B. Online Estimation and Error Analysis of both SOC and SOH of Lithium-ion Battery based on DEKF Method. *Energy Procedia* **2019**, *158*, 3008–3013. [CrossRef]

14. Wang, S.; Fernandez, C.; Yu, C.; Fan, Y.; Cao, W.; Stroe, D.I. A novel charged state prediction method of the lithium ion battery packs based on the composite equivalent modeling and improved splice Kalman filtering algorithm. *J. Power Sources* **2020**, *471*, 228450. [CrossRef]
15. Zhang, X.; Lu, J.; Yuan, S.; Yang, J.; Zhou, X. A novel method for identification of lithium-ion battery equivalent circuit model parameters considering electrochemical properties. *J. Power Sources* **2017**, *345*, 21–29. [CrossRef]
16. Lei, Z.; Zhang, C.; Li, J.; Fan, G.; Lin, Z. Preheating method of lithium-ion batteries in an electric vehicle. *J. Mod. Power Syst. Clean Energy* **2015**, *3*, 289–296. [CrossRef]
17. Liu, Y.; Zhang, R.; Hao, W. Evaluation of the state of charge of lithium-ion batteries using ultrasonic guided waves and artificial neural network. *Ionics* **2022**, *28*, 3277. [CrossRef]
18. Hu, J.; Sun, Z.; Gao, Y.; Li, P.; Wu, Y.; Chen, S.; Wang, R.; Li, N.; Yang, W.; Shen, Y.; et al. 3D stress mapping reveals the origin of lithium-deposition heterogeneity in solid-state lithium-metal batteries. *Cell Rep. Phys. Sci.* **2022**, *3*, 100938. [CrossRef]
19. Fang, S.; Yan, M.; Hamers, R.J. Cell design and image analysis for in situ Raman mapping of inhomogeneous state-of-charge profiles in lithium-ion batteries. *J. Power Sources* **2017**, *352*, 18. [CrossRef]
20. Migge, S.; Sandmann, G.; Rahner, D.; Dietz, H.; Plieth, W. Studying lithium intercalation into graphite particles via in situ Raman spectroscopy and confocal microscopy. *J. Solid State Electrochem.* **2005**, *9*, 132. [CrossRef]
21. Ghobakhloo, M. Industry 4.0, digitization, and opportunities for sustainability. *J. Clean. Prod.* **2020**, *252*, 119869. [CrossRef]
22. Ebadpour, M.; Jamshidi, M.B.; Talla, J.; Hashemi-Dezaki, H.; Peroutka, Z. Digital Twin Model of Electric Drives Empowered by EKF. *Sensors* **2023**, *23*, 2006. [CrossRef] [PubMed]
23. Braun, J.; Júnior, A.O.; Berger, G.; Pinto, V.H.; Soares, I.N.; Pereira, A.I.; Lima, J.; Costa, P. A robot localization proposal for the RobotAtFactory 4.0: A novel robotics competition within the Industry 4.0 concept. *Front. Robot. AI* **2022**, *9*, 1023590. [CrossRef] [PubMed]